



Precipitation and streamflow trends in Michigan, USA

J. E. Manzano¹ · B. D. Barkdoll¹

Received: 10 August 2021 / Accepted: 5 January 2022 / Published online: 5 March 2022
© The Author(s), under exclusive licence to Springer Nature Switzerland AG 2022

Abstract

Precipitation and streamflow trends may be changing due to changing climate. Therefore, data for these in the state of Michigan, USA, are examined through the use of statistical methods. Data from 117 precipitation stations were used, along with data from 143 streamflow gages. Data time periods varied among the stations with the longest record dating back to 1901. These methods include the linear regression best-fit line for the whole data set and also for before and after a two-sample change point analysis, moving mean, and moving standard deviation. It was found that mean precipitation for 90% of the locations and mean streamflow for 76% of the locations increased over the period of record. The moving standard deviation for precipitation increased for 54% of the locations, while 28% of the streamflow locations had an increase. Values of precipitation $P(T \leq t)$ two-tail, precipitation linear regression slope, and streamflow $P(T \leq t)$ two-tail at a 0.05 significance level occur in concentrated regions. 97% of the precipitation data sets and 92% of the streamflow data sets exhibited a distinct change. These results have implications for future management of flood control, recreation, water supply, and irrigation.

Keywords Water resources · Climate · Weather · Watershed · Hydrology

Abbreviations

MI	Michigan, USA
NOAA	National Oceanic and Atmospheric Administration
NWS	National Weather Service
TUW	Lumped rainfall–runoff model with the structure of the HBV model (Lindström 1997)
U,P	Upper Peninsula of Michigan
USGS	United States Geographic Survey
WFO	Weather Forecast Office

Introduction

State of Michigan geography and climate

Michigan is located in the Northern US, centrally located east to west (Fig. 1). Michigan has two parts, or peninsulas, northern and southern. The southern peninsula is surrounded by Lake Michigan on the west and Lake Huron to the east. It is north of the states of Indiana and Ohio. The Northern

Peninsula or sometimes called the Upper Peninsula (U.P.) is disconnected from the lower peninsula by the portion of lake that connects Lakes Michigan and Huron. The U.P. is connected to the state of Wisconsin to the south and Lake Superior to the north.

The climate is characterized as a Humid Continental Climate (NWS 2021), which means that it has distinct seasons and an annually even rainfall distribution throughout the year. The mean annual temperature ranges from 24.5° Fahrenheit in January to 73.5° in July for the largest city of Detroit, located in the southern portion of the Lower Peninsula. Precipitation is primarily snow in the winter, while showers and thunderstorms are frequent in the summer. Michigan is unique in that it is significantly surrounded by Great Lakes and is therefore particularly subjected to precipitation and related streamflow phenomenon. Michigan has 5292 km (3288 miles) of freshwater shoreline, thereby making it the state with the most such shoreline in the US (State of Michigan 2021).

Literature review of precipitation and streamflow trends

There have been several studies on precipitation and streamflow, a partial list of the most recent and most relevant of which is in Table 1. Of note is that of Hagedorn and

✉ B. D. Barkdoll
barkdoll@mtu.edu

¹ Michigan Technological University, Houghton, MI 49931, USA

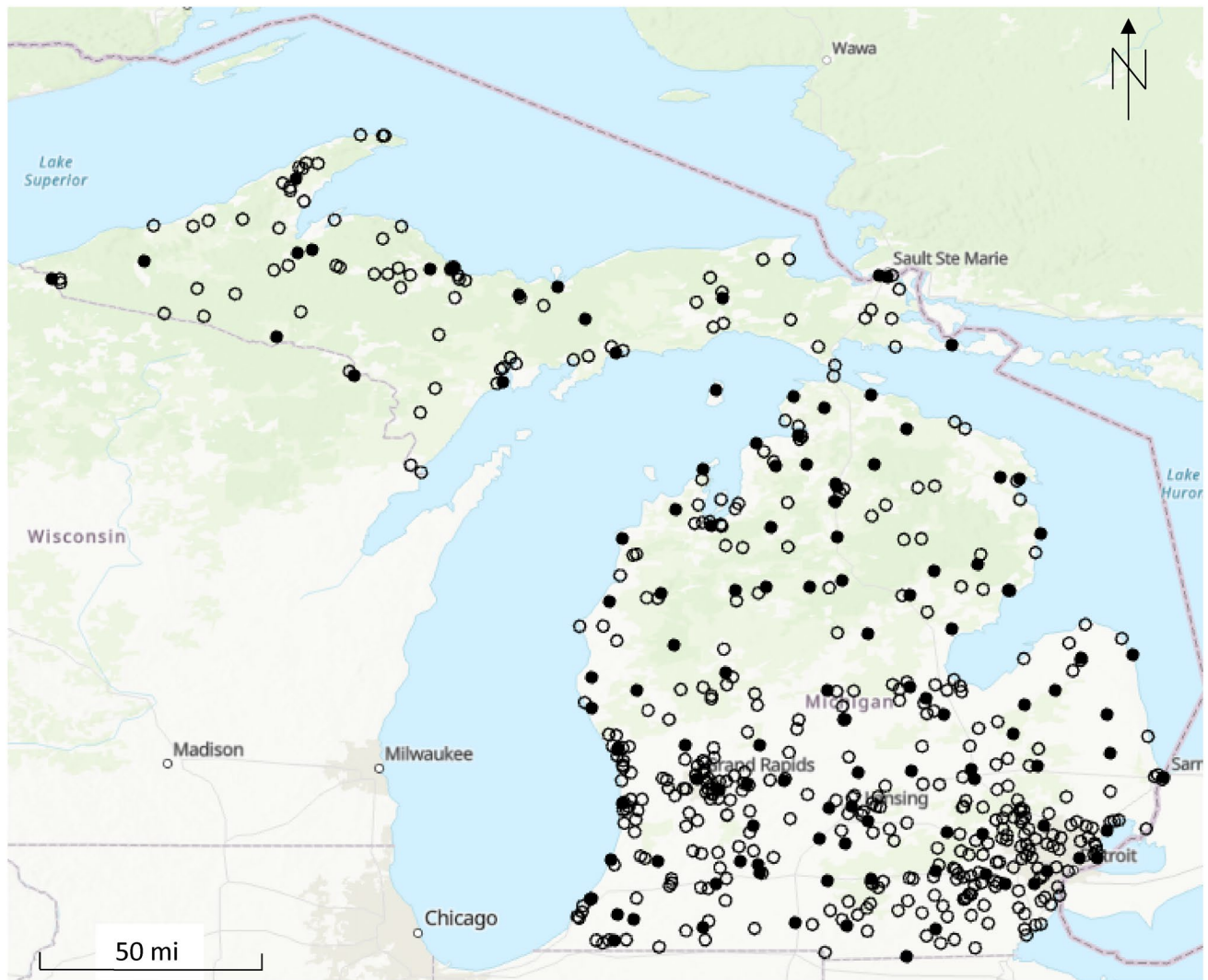


Fig. 1 All precipitation stations in Michigan (solid black dots represent stations with more than 20 data points; hollow dots represent neglected stations due to insufficient data. Study area is where dots occur.)

Meadows (2021) which studied only the undisturbed watersheds in Michigan. The current study is unique in studying all the Michigan watersheds.

Study purpose

The purpose of this study is to analyze the trends for precipitation and streamflow throughout the State of Michigan to shed light on the following questions:

1. Are precipitation and streamflow increasing, as shown by increasing linear trend lines of the data?
2. Are the extremes of precipitation and streamflow increasing, as shown by increasing slopes of the moving average and moving standard deviation of the data?

These questions have implications for future management of watershed for flooding, transportation, recreation, and water supply. The novelty of this work is that nobody has done this kind of analysis for the State of Michigan before.

Materials and methods

Description of data

The state of Michigan has 548 precipitation stations, as shown in Fig. 1. There are multiple types of precipitation stations with some measurements taken automatically and some manually (NOAA 2021). Within all Michigan watersheds, there are 209 streamflow gaging stations, as shown in Fig. 2. Streamflow gaging stations are managed by the U.S.

Table 1 Recent and relevant studies on precipitation and stream flow trends

Citation	Location	Precip	Strmfl
Adib and Tavancheh (2019)	Kelani River basin, Sri Lanka	X	X
Al-Hasani (2019)	Tigris River Basin, Iraq		X
Ali et al. (2019)	Yangtze River, China		X
Asarian and Walker (2016)	NW California and SW Oregon	X	X
Balistrocchi et al. (2021)	Central Italian alps	X	X
Darlane and Pouryafar (2021)	Zarrinehrood River basin in Iran		X
Fleming et al. (2021)	Chesapeake Bay	X	X
Fooladi et al. (2021)	Shahpour River basin in the south of Iran	X	X
Guo et al. (2018)	Gongshui River, China		X
Gu et al. (2021)	China	X	X
Gupta et al. (2020)	Jharkhand state, India	X	
Hagedorn and Meadows (2021)	Undisturbed watersheds in Michigan		X
Henn et al. (2018)	Sierra Nevada	X	X
Kelly et al. (2016)	Unstated	X	X
Kuriqi et al. (2020)	Central India		X
Lee and Yeh (2019)	River basins in northern Taiwan	X	X
Leuthold et al. (2021)	S.W. Montana	X	X
Lucas et al. (2021)	Sao Francisco river basin, Brazil	X	X
Ma et al. (2019)	S.W. China	X	X
Mallakpour et al. (2018)	California		X
Nkhonjera et al. (2021)	Olifants River basin, Africa	X	
Penn et al. (2020)	Rio Grande headwaters	X	X
Shrestha et al. (2021)	Permafrost region, Canada		X
Sidibe et al. (2018)	West and Central Africa		X
Swain et al. (2021)	Brahmani, Baitarani R. catchments, E. India		X
Talchabhadel et al. (2021)	West Rapti River basin, Nepal	X	X
Tan and Gan (2017)	Canada	X	X
Tan et al. (2021)	Yarlungzangbo River, Tibet		X
Vijay et al. (2021)	Kerala, India	X	
Wen et al. (2021)	Huai river basin, China	X	X
Xu et al. (2021)	Amu Darya River Basin, Central Asia		X
Yan et al. (2017)	Miyun Reservoir Basin, China	X	X
Zeľeňáková et al. (2017)	Košice, Slovakia	X	
Zeng et al. (2021)	US		X
Zhang et al. (2017)	Upper Sang-kan basin, China	X	X
Zhang et al. (2020)	Loess Plateau, China	X	X
Zhong et al. (2021)	Yellow R., China		X

Geological Survey (USGS) and measure the water elevation which is used in conjunction with a stage-streamflow rating curve to calculate the streamflow (USGS 2021a). It can be seen that the spatial coverage of measurement stations is broad. Only data sets with 20 or more data points were used, to ensure meaningful statistical value.

Methods

All available precipitation data from the first year of record for a particular precipitation station were obtained from the National Oceanic and Atmospheric Administration (NOAA)

online weather database for all precipitation stations in Michigan (NOAA 2021). All available streamflow data were obtained from the United States Geological Survey (USGS) website for all Michigan Watersheds dating back to 1901 (USGS 2021b). Precipitation and streamflow stations with fewer than 20 data points were discarded, since they contain insufficient data.

The mean, standard deviation, and coefficient of variation of all data were calculated and recorded for each station. These data were plotted as precipitation over time for each individual station and the slope linear regression slope was recorded. The slope of the linear regression line represents a

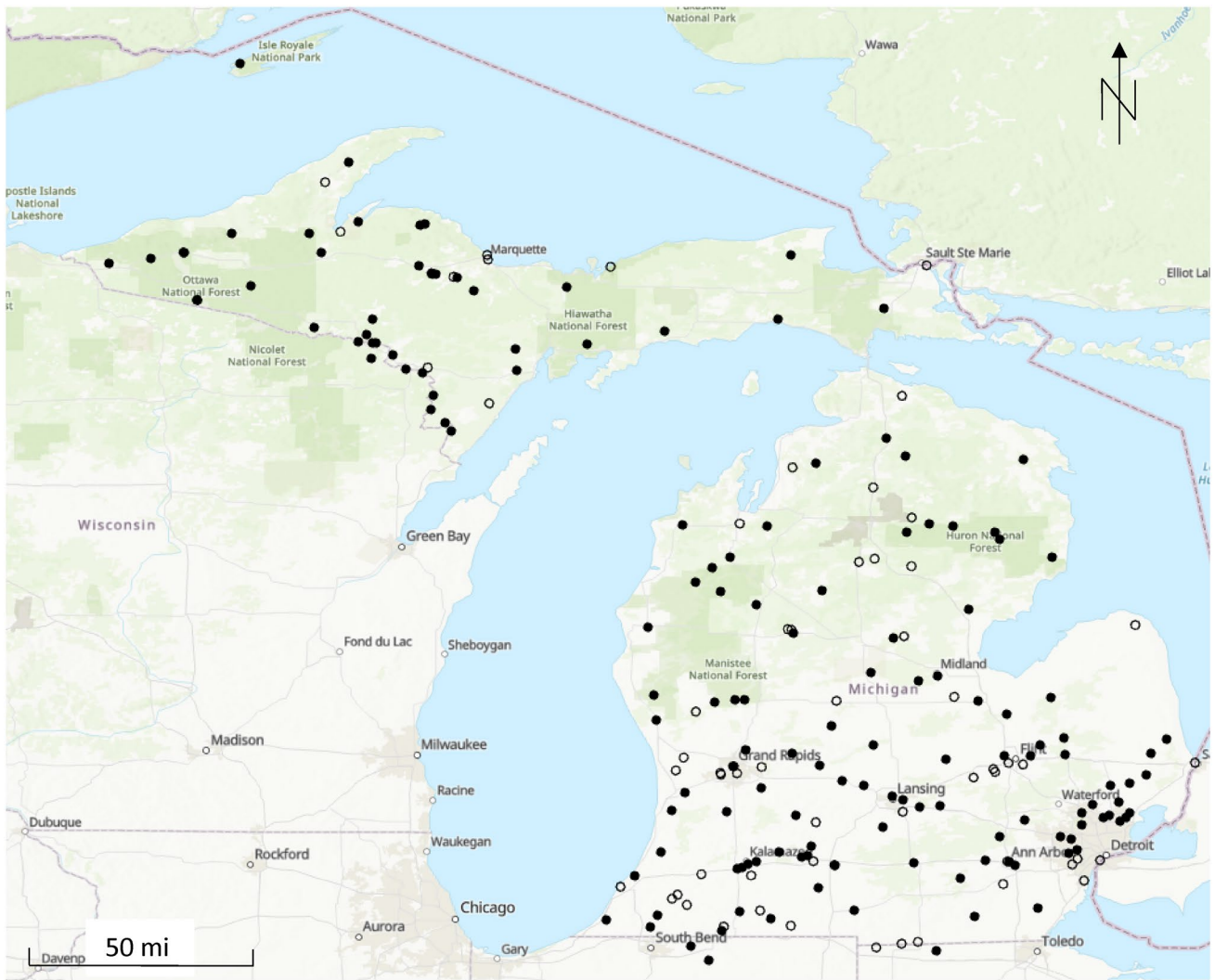


Fig. 2 All streamflow gaging stations in Michigan watersheds (solid black dots represent stations with more than 20 data points; hollow dots represent neglected stations due to insufficient data. Study area is where dots occur.)

long-term trend. An assumption of linear regression is normality, which may introduce some error in the regression line slope values. Future analysis can be done with the Mann–Kendal test, for example, that does not assume normality. When the nonparametric Theil–Sen slope estimator is applied, instead of linear regression, the results are similar to linear regression on streamflow data (Wasko et al. 2020). Trend were sought, however, not exact values for predictive purposes. The number of stations with positive slopes (increasing trends) was counted and expressed as a percentage of the total number of stations that contain more than 20 precipitation data points. The 11-day moving average (also a metric of long-term trends) and moving standard deviation, which is a metric of long-term trends in extreme values, were calculated as well. These are hereafter referred to as the “moving statistics.” The moving statistics were also plotted over time for

each individual station and the slope of their linear regressions were recorded. Again, the number of positive slopes between all of the stations was summed and expressed as a percentage of the total amount of pertinent precipitation stations.

To investigate the presence of change points in precipitation and streamflow, a two-sample change point analysis using a visual inspection was performed to identify the appropriate point in the given data set that best represents a split in the data. A change point is defined here as a point in time where a change in trends occurred. The change could be from a lower slope to a higher one or vice versa. For some cases, this point was chosen to be where data gaps exist, if any. The prefixes “pre” and “post” were used to identify the data prior to and after, respectively, the determined change point. T tests that assume unequal variances were conducted for all pertinent precipitation and streamflow stations using the Excel spreadsheet

T test function. The t test also assumes normally distributed data, which may not be true here. The hypothesized mean difference was set to zero, since it was assumed that the “pre” and “post” data for each station originate from the same data set. Alpha, the correlation coefficient, was set to equal 0.05, since it is a commonly accepted value for statistical analysis. The amount of precipitation and streamflow stations that had $P(T \leq t)$ two-tail values less than 0.05 were counted and expressed as a percentage of the total amount of t tests performed. The amount of t Stat values greater than t Critical two-tail values was also counted, as well as the amount of stations that had both the $P(T \leq t)$ two-tail values less than 0.05 and t Stat values greater than t Critical two-tail values. These summations were both expressed as a percentage of the total amount of t tests that were conducted. The plots of streamflow over time were examined and unnatural data sets were flagged. This included data that appeared to be cyclic and/or not scattered. The amount of flagged data sets was recorded. Change point analysis assumes a sudden change, which may or may not be true for climate change. The climate is changing more gradually due to the increase in greenhouse gas emissions. Nevertheless, many studies have used change point analysis to gage trends in data.

A contour map was created of the precipitation $P(T \leq t)$ two-tail values obtained from the t tests and of the slope of the linear regression line of the dataset for each station. In order to construct this, the latitude and longitude coordinates of each precipitation station were taken from the NOAA “Find a Station” data tool webpage. The $P(T \leq t)$ two-tail and linear regression slope contour maps use a contour interval of 0.05 and 0.01, respectively, while the respective amount of color classes for each contour map are 5 and 32. Each streamflow gaging station was examined to determine if any upstream dams exist that would potentially affect the streamflow data. Any notable structures were recorded with the corresponding gaging station.

A compilation was created of all Michigan watershed maps. A map of the state of Michigan was shown alongside each watershed map with the location of the watershed marked. The gaging stations within each watershed were marked as were any dams and rivers/streams. An arrow was placed pointing to each gaging station to identify the corresponding slope of the linear regression of the streamflow data for each location. These are all given in the Supplemental Information related to this article.

Results

Precipitation

In total, there are 548 precipitation stations within the state of Michigan. Of these 548 stations, 117 have at least

20 data points. The precipitation station at the Marquette Weather Forecast Office (WFO) in Michigan will be used as an example in the following results as it is a good representation with an ample amount of data and it is located relatively close to the streamflow gaging station that was used as an example in Sect. 3.2.

The mean of all precipitation data points for each station ranges from 28.46 inches in Houghton Lake, MI, to 40.34 inches in Niles, MI. The lowest standard deviation is found at the Gaylord Otsego County Airport in Michigan at 3.22 inches, while the highest standard deviation is 7.02 inches in Herman, MI. The Gaylord Otsego County Airport station also has the lowest coefficient of variation of precipitation data at 0.11, while the largest coefficient of variation is 0.21 at the Harbor Beach 1 SSE, MI, station. Figure 3 shows the precipitation data plot for the Marquette WFO, MI, station. This type of plot was created for all 117 gaging stations and can be found. The linear regression for this particular location displays a slope of 0.0902 in/year.

Of all precipitation stations, the slope of the linear regressions ranged from -0.1448 in/year in Morenci, MI, to 0.4039 in/year at the Gaylord 9SSW, MI, station. Positive linear regression slopes appear to be in 89.74% of the stations. When this slope is divided by the average streamflow of each particular location and multiplied by 100, both of these stations, respectively, had the smallest and largest value of this statistic with the smallest being -0.3860 /year and the largest being 1.0532 /year. It was found that 89.74% of the 117 stations had positive values of linear regressions divided by average streamflow values.

After calculating the 11-day precipitation moving averages, moving standard deviations, and moving coefficient of variations, it was seen that 46 stations had at least 20 data points and could be further evaluated. The slope of the linear regressions for moving average data sets ranged from -0.0891 in/year at the Pellston Regional Airport in Michigan to 0.2671 in/year at the Caro Wastewater Treatment Plant in Michigan. Additionally, 76.09% of the 46 stations had positive linear regression slopes for moving averages. The moving standard deviation linear regression slopes ranged from -0.1465 in/year at the Manistee 3SE, MI, station to 0.1262 in/year at the Detroit City Airport in Michigan. Out of the 46 precipitation stations, 54.35% of them had positive linear regression slopes for the moving standard deviations. The Manistee 3SE, MI, station and the station at the Detroit City Airport both also have the smallest and largest slope of moving coefficient of variation regression at -0.0053 /year and 0.0040 /year, respectively. Of the 46 precipitation stations, 41.30% had positive linear regression slopes for moving coefficient of variations.

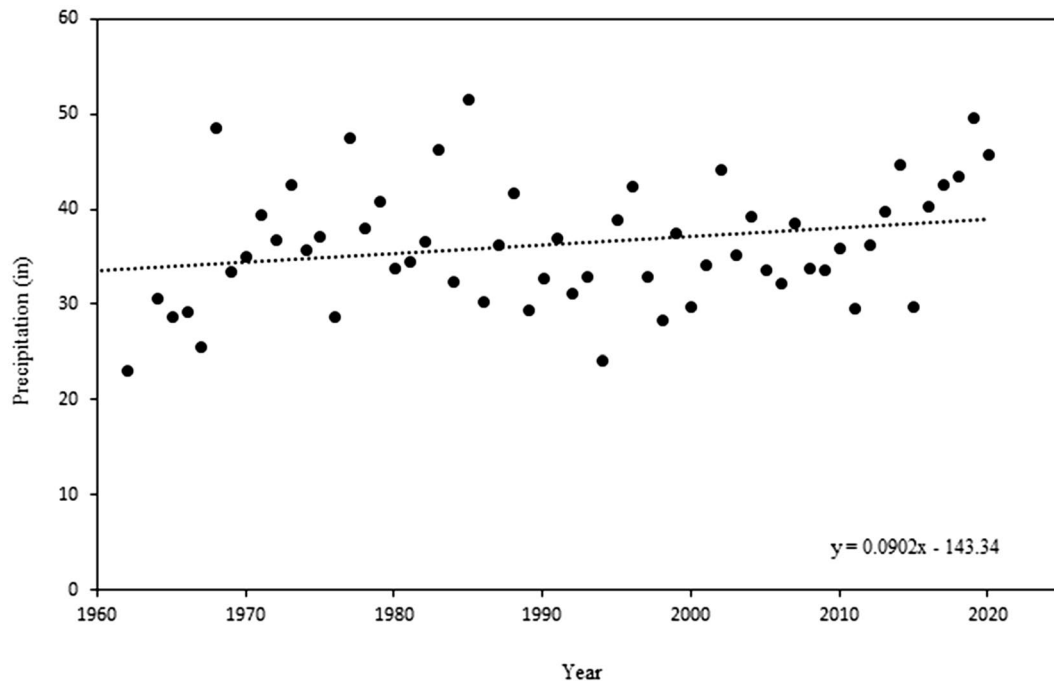


Fig. 3 Precipitation data for the example station at Marquette WFO, MI

An example of splitting the data into two datasets based on a visual inspection of changing slopes is shown in Fig. 4 for the Marquette WFO, MI, station. For this example, the “pre” data have a slope of 0.5679 in/year and the “post” data exhibit a slope of 0.2634 in/year. This

corresponds to a change of 53.62%. The mean percentage of change between all of the “pre” and “post” precipitation slopes was found to be -123.13% . Table 2 displays the results of the t test for this precipitation station, where the first three rows of column one are for the “pre” data

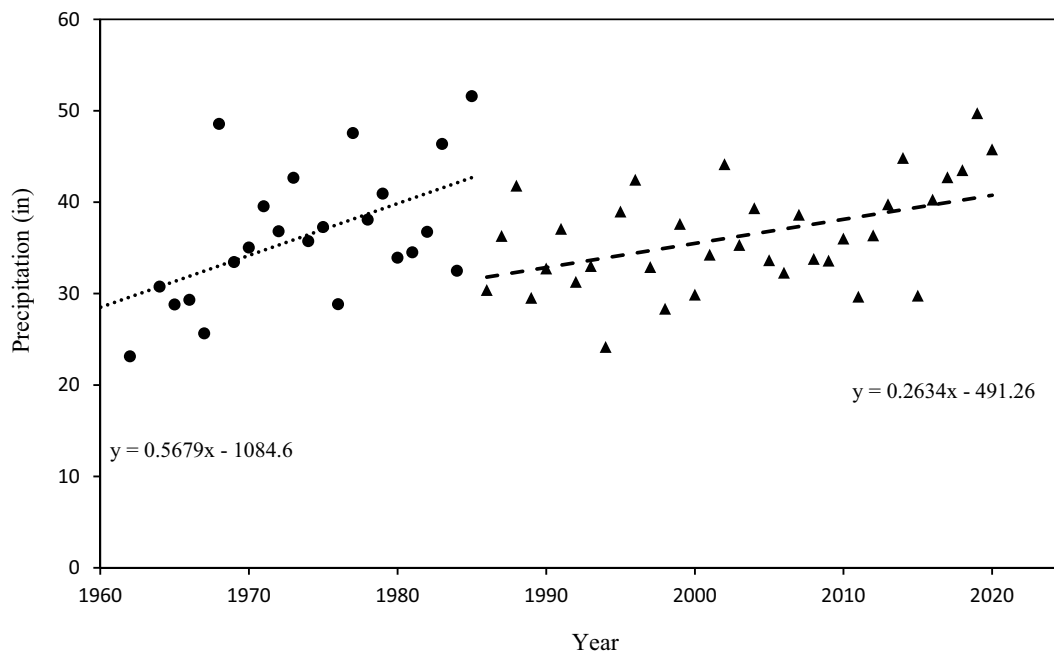


Fig. 4 “Pre” (circle) and “post” (triangle) precipitation data for the example station at Marquette WFO, MI

Table 2 Precipitation T test results for the example station at Marquette WFO, MI

Statistic	Pre-data set	Post-data set
Mean	36.42	36.28
Variance	54.58	33.49
Observations	23	35
Hypothesized mean difference	0	
df	39	
t Stat	0.0764	
$P(T \leq t)$ one-tail	0.4697	
t Critical one-tail	1.6849	
$P(T \leq t)$ two-tail	0.9394	
t Critical two-tail	2.0227	

and the first three rows of column two are representative of the “post” data. A summary of all the statistics for all precipitation gage locations is given in Table 3.

In total, there were 43 precipitation stations, or 36.75%, that had $P(T \leq t)$ two-tail values less than 0.05. Three of these stations also had t Stat values greater than t Critical two-tail values; therefore, the hypothesis that the data of each individual precipitation station come from a singular dataset is rejected for 2.56% of the 117 precipitation stations that t tests were run for.

Figure 5 shows the contour map that was created using all of the obtained precipitation $P(T \leq t)$ two-tail values. Similarly, Fig. 6 shows the contour map that was created using the slope of the linear regression of each station’s precipitation values.

Table 3 Summary of precipitation statistical results for all gages

Statistic	$n > 20$ count	% Gages $m > 0$	μ_m count	% Gages $\mu_m > 0$	% Gages $\sigma_m > 0$	% Gages increasing trend in pre and post m values
Value	117	90	46	89	79	39

μ_m 11-day moving average, σ_m 11-day moving standard deviation

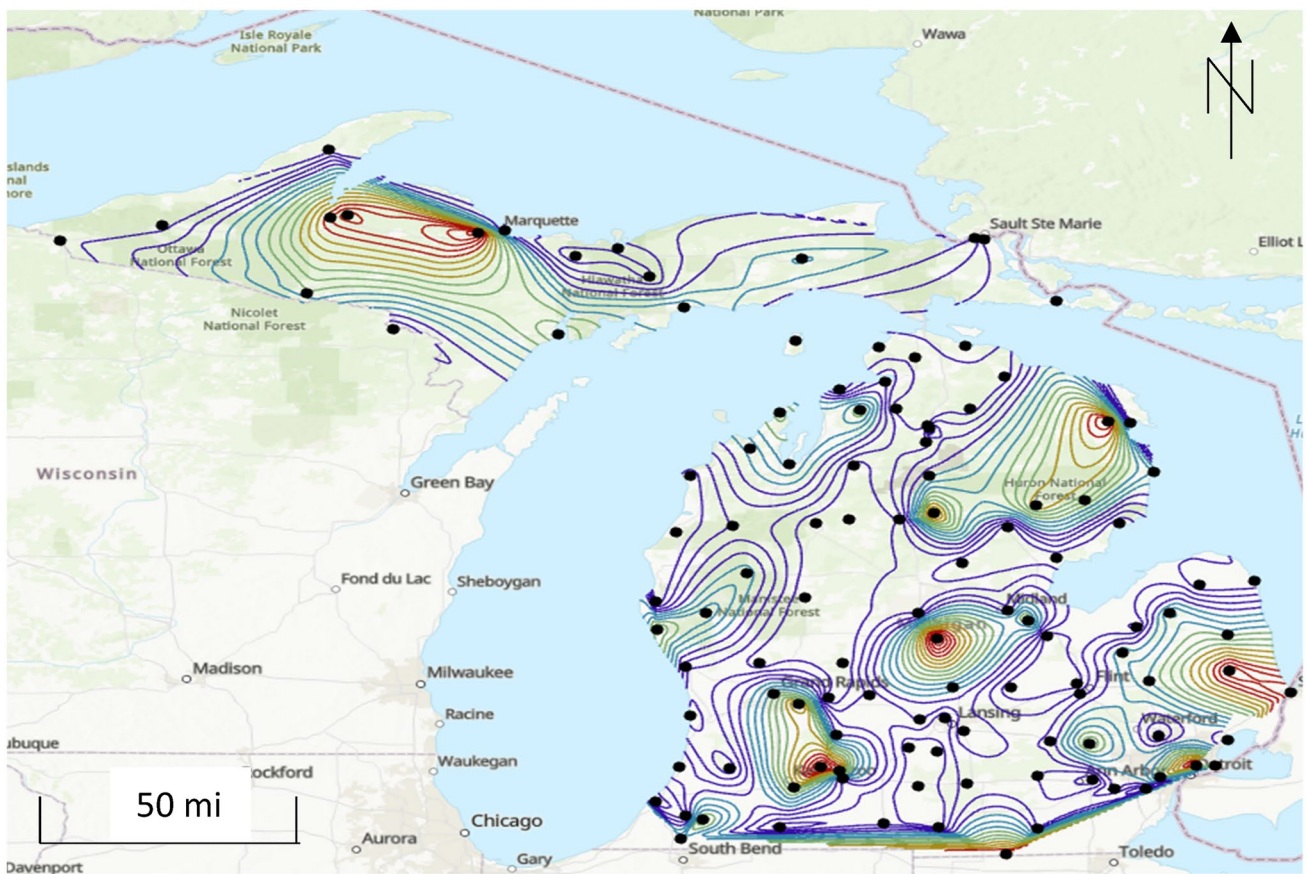


Fig. 5 Contour map of precipitation $P(T \leq t)$ two-tail values (each black dot is a precipitation station and the contour lines are colored with the red lines representing the highest $P(T \leq t)$ two-tail values and the purple lines representing the lowest. Study area is where dots occur.)

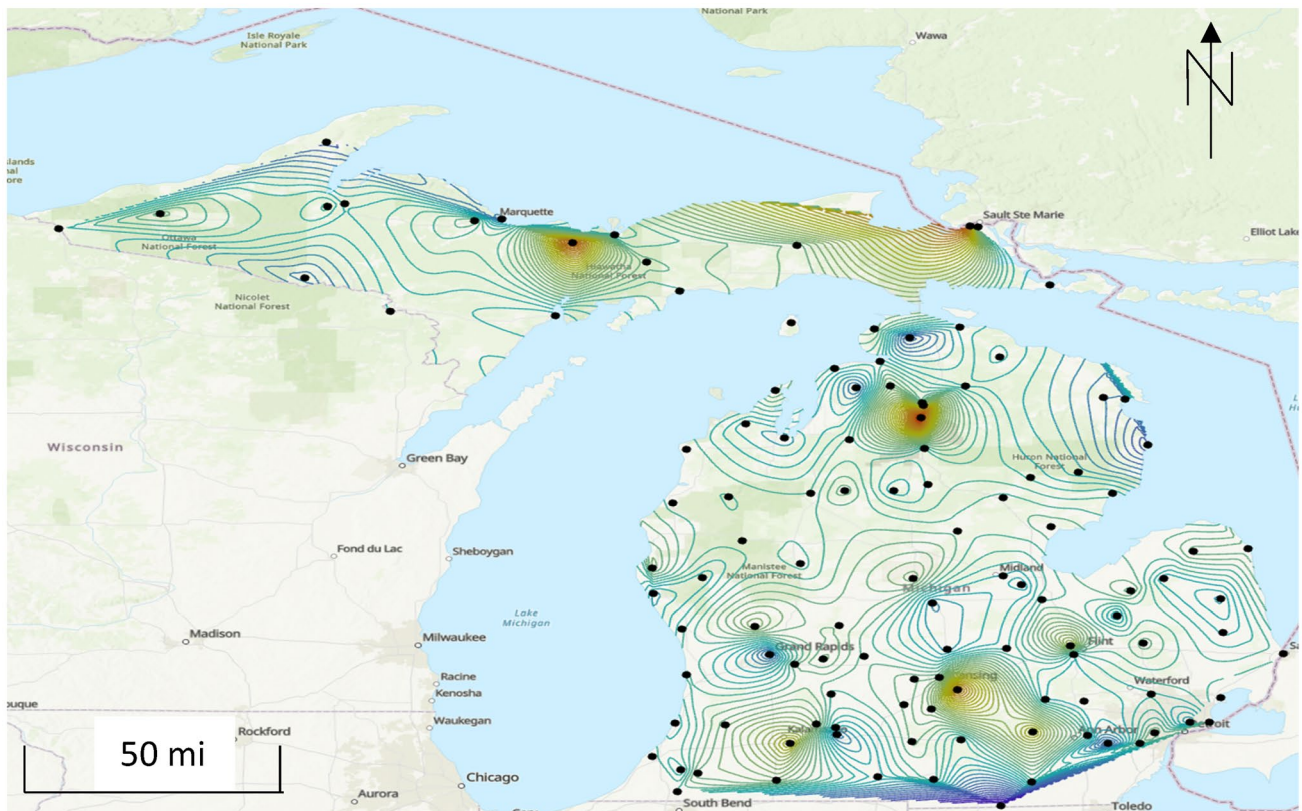


Fig. 6 Contour map of precipitation linear regression slope values (the red contour lines represent the highest values, while the purple contour lines represent the lowest. Study area is where dots occur.)

A map of the Escanaba River Basin is shown in Fig. 7 with the precipitation stations marked. Each station is labeled and those that had enough data include the value of the slope of the linear regression of the respective station's data.

Streamflow

In total, there are 209 streamflow gages in Michigan watersheds. Of these 209 gages, 143 of them have at least 20 data points. The Escanaba River Basin will be used as an example in the following results as it is a good representation with multiple streamflow gaging stations and dams. The analysis for all watershed is given in the supplemental data.

The mean of all streamflow data points for each gaging station ranges from 5.59 ft³/s in Oshtemo, MI, to 4831.24 ft³/s in Saginaw, MI. These same gaging stations also hold the lowest and highest standard deviations of 0.79 ft³/s and 1224.69 ft³/s, respectively. The lowest coefficient of variation of streamflow data is found in East Jordan, MI, at 0.05 while the highest is found in Palmer, MI, at 0.48. Figure 8 shows the streamflow data plot for gaging station 04057800 in the Middle Branch Escanaba River located in Humboldt, MI. This type of plot was created for all 143 gaging stations and can be found in

the supplemental information. The linear regression for this particular location displays a slope of -0.1822 cfs/year.

Of all streamflow gaging stations, the slope of the linear regressions ranged from -5.7041 cfs/year in Pembine, WI, to 46.09 cfs/year in Banat, MI. Positive linear regression slopes appear to be in 75.68% of the gages. When this slope is divided by the average streamflow of each particular location and multiplied by 100, the minimum of this statistic is found in Oshtemo, MI, with a value of -2.2064 /year. This is the same gaging station that exhibits the smallest average streamflow and standard deviation and also has the smallest value of regression slope divided by mean streamflow. This same relationship does not exist for the largest statistic of linear slope divided by mean streamflow; this is found in Hastings, MI, and holds a value of 2.6554/year. It was found that 74.58% of the 143 gaging stations had positive values of linear regressions divided by average streamflow values.

After calculating the 11-day streamflow moving averages and moving standard deviations, it was seen that 118 gaging stations had at least 20 data points and could be further evaluated. The slope of the linear regressions for moving average data sets ranged from -25.767 cfs/year in Pembine, WI, to 18.0 cfs/year in Grand Rapids, MI. The location in Pembine is the same gaging station that had the linear regression with

Escanaba River Basin

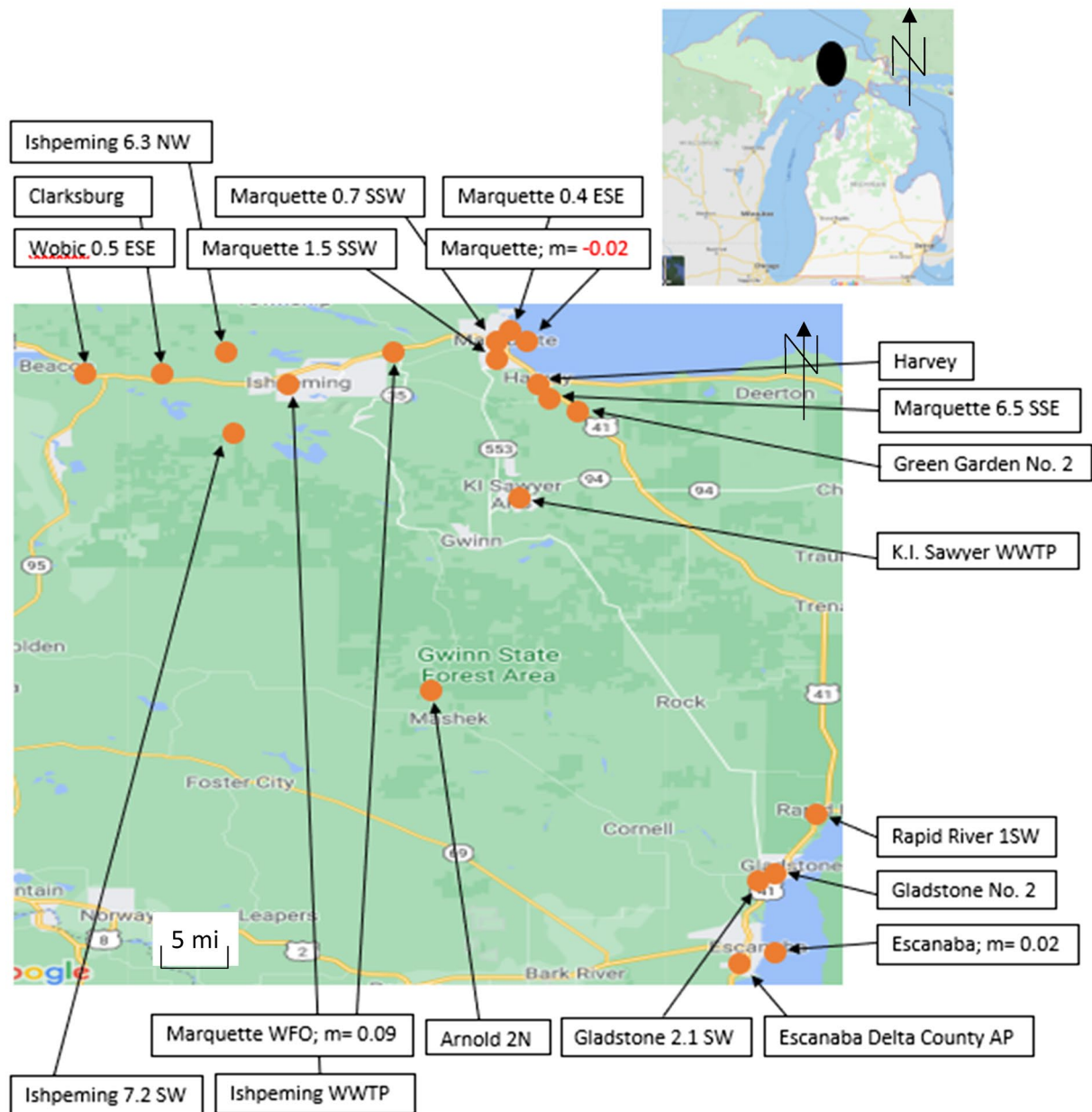


Fig. 7 Escanaba River Basin precipitation values of the slope of the linear regression values, m , for those gages that had sufficient data (Google Maps)

the smallest slope from the raw data. Additionally, 66.10% of the 118 gages had positive linear regression slopes for moving averages. The moving standard deviation linear regression slopes ranged from -7.3222 cfs/year at the same Pembine location to 5.0578 cfs/year in Vulcan, MI. This gaging station in Vulcan is in the Menominee River, which is the same river that the Pembine gage is in. Out of the 118 gages, 27.97% of them had positive linear regression slopes for the moving

standard deviations. The smallest slope of moving coefficient of variation regressions is -0.0081 /year in Birmingham, MI, while the largest is 0.0047 /year in Palmer, MI. This gaging station in Palmer is the same one that had the largest coefficient of variation of its raw data. Of the 118 gages, 33.05% had positive linear regression slopes for moving coefficient of variations.

There were 29 data sets that appeared to have cyclic/unnatural streamflow data, perhaps due to a dam gate opening and

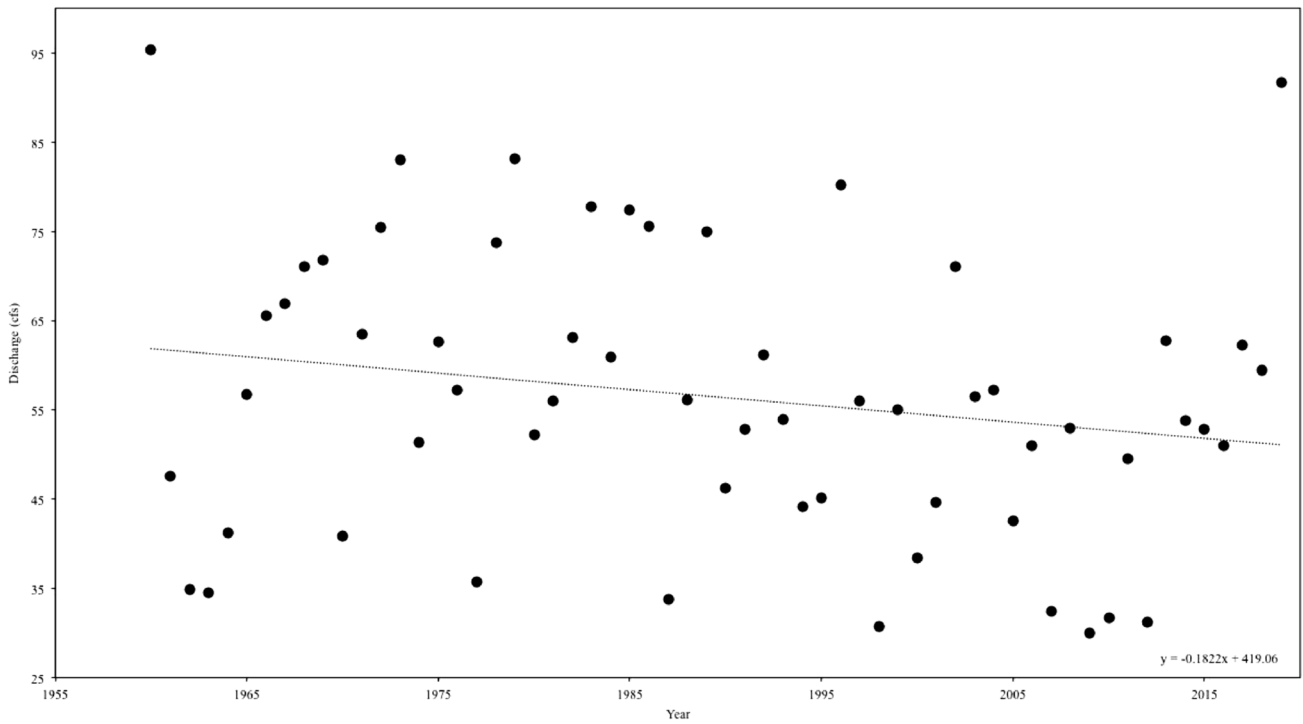


Fig. 8 Streamflow data for gage 04,057,800 in the Middle Branch Escanaba River located in Humboldt, MI

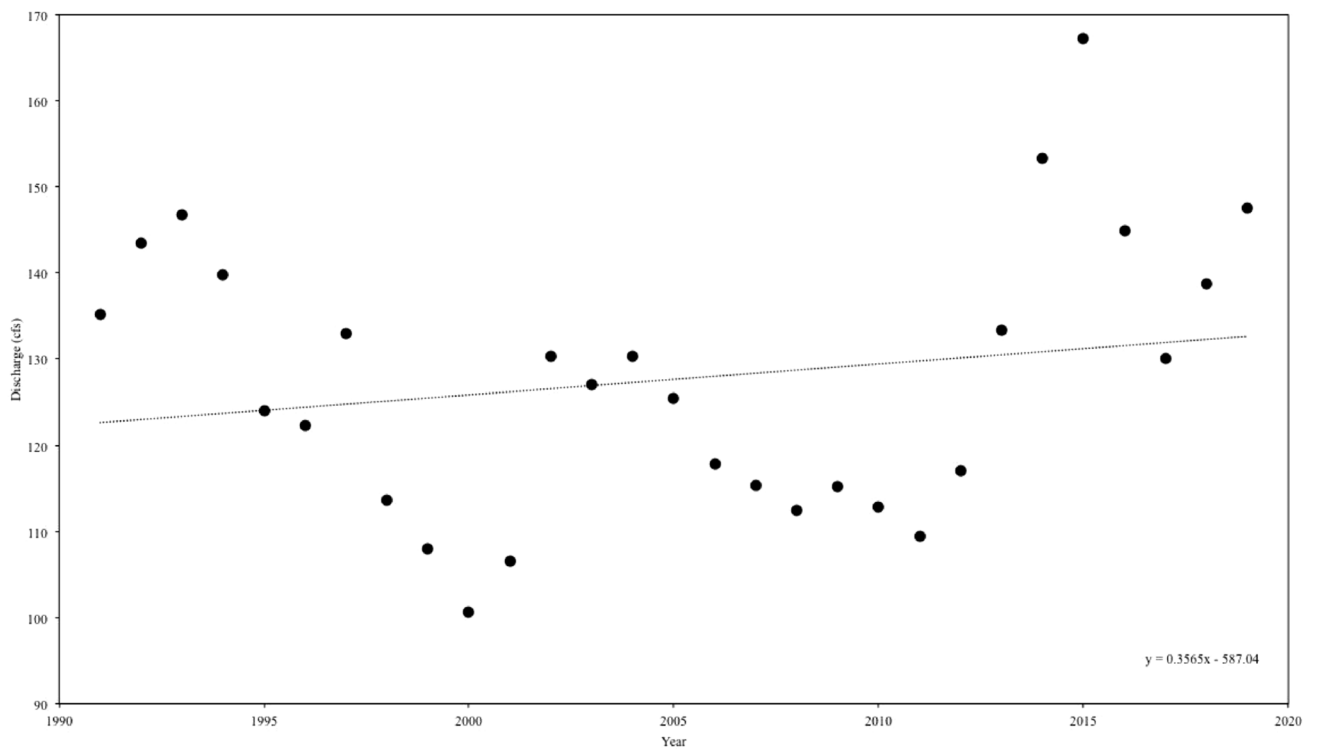


Fig. 9 Example of cyclic data of streamflow at gage 04126740

Fig. 10 “Pre” (circle) and “post” (triangle) streamflow data for gage 04057800 at Mid Branch of the Escanaba River at Humboldt, MI

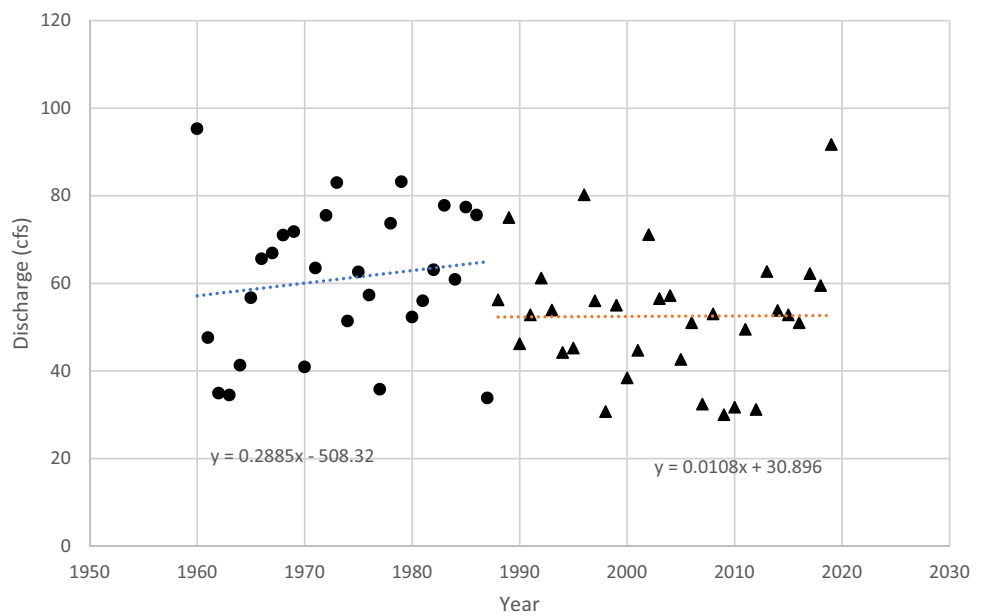


Table 4 Streamflow *T* test results for gage 04057800

Statistic	Pre-data set	Post-data set
Mean	61.05	52.49
Variance	278.89	205.10
Observations	28	32
Hypothesized mean difference	0	
<i>df</i>	54	
<i>t</i> Stat	2.1200	
$P(T \leq t)$ one-tail	0.0195	
<i>t</i> Critical one-tail	1.6700	
$P(T \leq t)$ two-tail	0.0389	
<i>t</i> Critical two-tail	2.0000	

closing according to some set algorithm. Regardless, these do exist for a percentage of the total gaging stations and it should be noted. An example of this data is shown in Fig. 9.

An example of splitting the data into two datasets based on a visual inspection of changing slopes is shown in Fig. 10 for gaging station 04057800 in the Middle Branch Escanaba River located in Humboldt, MI. For this example, the “pre” data have a slope of 0.2885 cfs/year and the “post” data exhibit a slope of 0.0108 cfs/year. This corresponds to a change of 96.26%. The mean percentage of change between all of the “pre” and “post” streamflow slopes was found to

be 252.65%. Table 4 displays the results of the *t* test for this gaging station. A summary of all the statistics for all streamflow gage locations is given in Table 5.

In total, there were ten streamflow gaging stations, or 7.09%, that had $P(T \leq t)$ two-tail values less than 0.05. All ten of these gaging stations also had *t* Stat values greater than *t* Critical two-tail values. Therefore, the hypothesis that the data of each individual streamflow gaging station come from a singular dataset is rejected for 7.09% of the 141 streamflow gaging stations that *t* tests were run for. Figure 11 shows the contour map that was created using all of the obtained streamflow $P(T \leq t)$ two-tail values.

Twenty percent of streamflow gaging stations were found to have nearby dams. It is possible that these dams impact the streamflow data and any related calculations.

The Escanaba watershed is shown in Fig. 12. The streamflow gaging stations are pointed out with their respective values of the slope of the linear regression for particular streamflow gaging station.

Discussion

The results of this study, namely that precipitation is increasing, agree with climate change theory that says there will be more precipitation in this region of the world as the climate

Table 5 Summary of streamflow statistical results for all gages

Statistic	$n > 20$ count	% Gages $m > 0$	μ_m count	% Gages $\mu_m > 0$	% Gages $\sigma_m > 0$	% Gages increasing trend in pre and post m values
Value	143	75	118	60	28	31

μ_m 11-day moving average, σ_m 11-day moving standard deviation

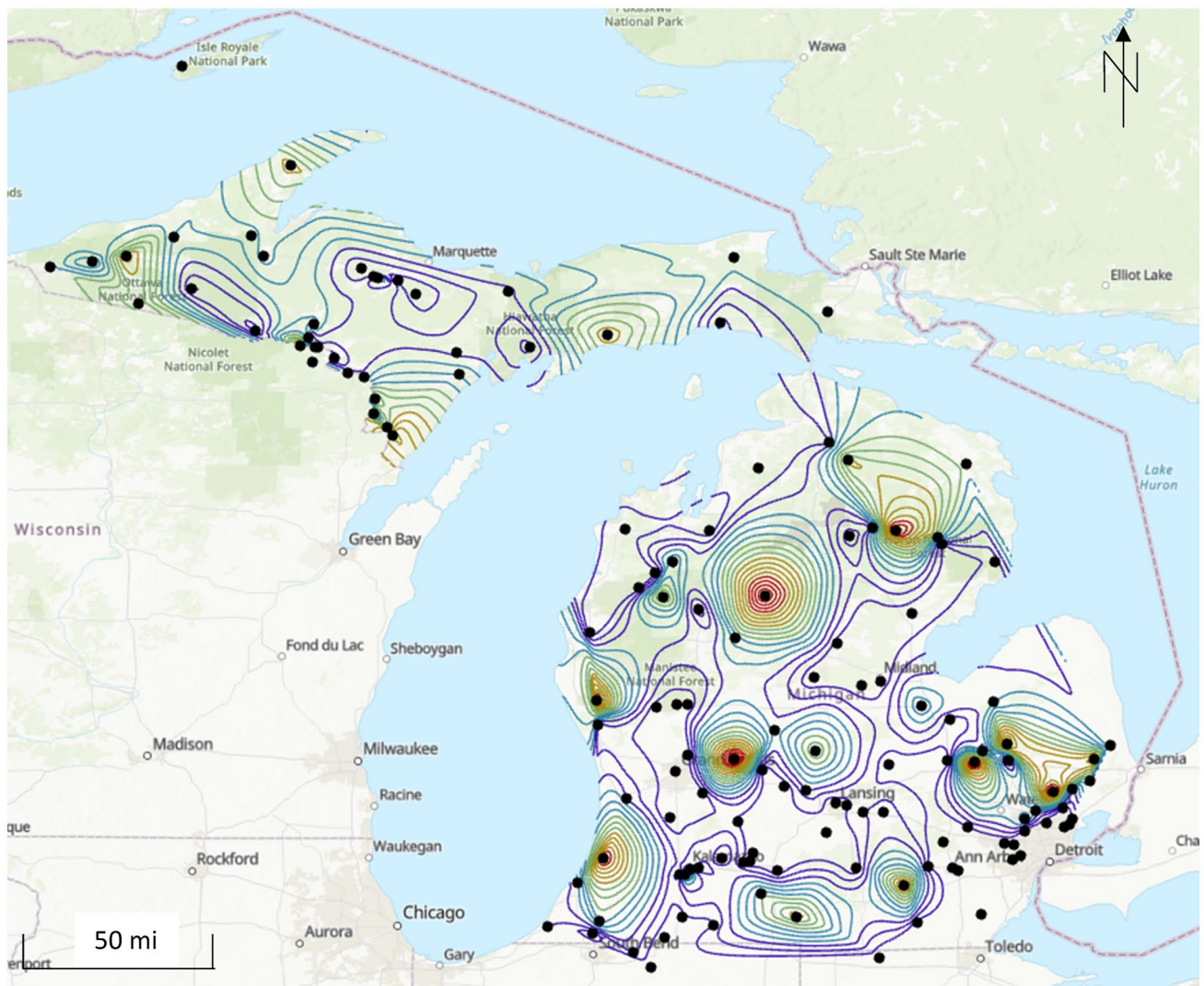


Fig. 11 Contour map of streamflow $P(T \leq t)$ two-tail values (each black dot is a streamflow gaging station and the contour lines are colored with the red lines representing the highest $P(T \leq t)$ two-tail values and the purple lines representing the lowest)

warms. The results the river flowrate is not increasing agrees with hydrology theory in that surface storage is able to absorb some of the increased precipitation.

This study quantified changing trends in precipitation and streamflow using the statistical methods of the linear regression best-fit line for the whole data set and also for before and after a change point, moving mean, and moving standard deviation. There are other statistical methods that could have been used and were used in other studies. These include frequent patterns mining and Random Forest methods (Zeng et al. 2021), the Budyko hypothesis and the TUW model (Zhong et al. 2021), the annual time series of 7-day average minimum streamflow, the scaled average deficit at or below the 2% mean daily streamflow value relative to a base period, and the annual number of days below the 2% threshold (Fleming et al. 2021), different

nonparametric Mann–Kendall trend tests (Adib and Tavancheh 2019; Yan et al 2017; Asarian and Walker 2016), gridded data set comparison (Henn et al. 2018), Mann–Kendall and Pettitt's test and double mass curve method (Guo et al. 2018), multiple linear regression (Shrestha et al. 2021), wavelet transfer methods (Zhanget al. 2017), detrended fluctuation analysis and multifractal DFA (Tan and Gan 2017), and m-DMC and m-SCARQ approaches (Swain et al. 2021).

Conclusions

A statistical analysis of all precipitation and streamflow data for the entire state Michigan shows the following:

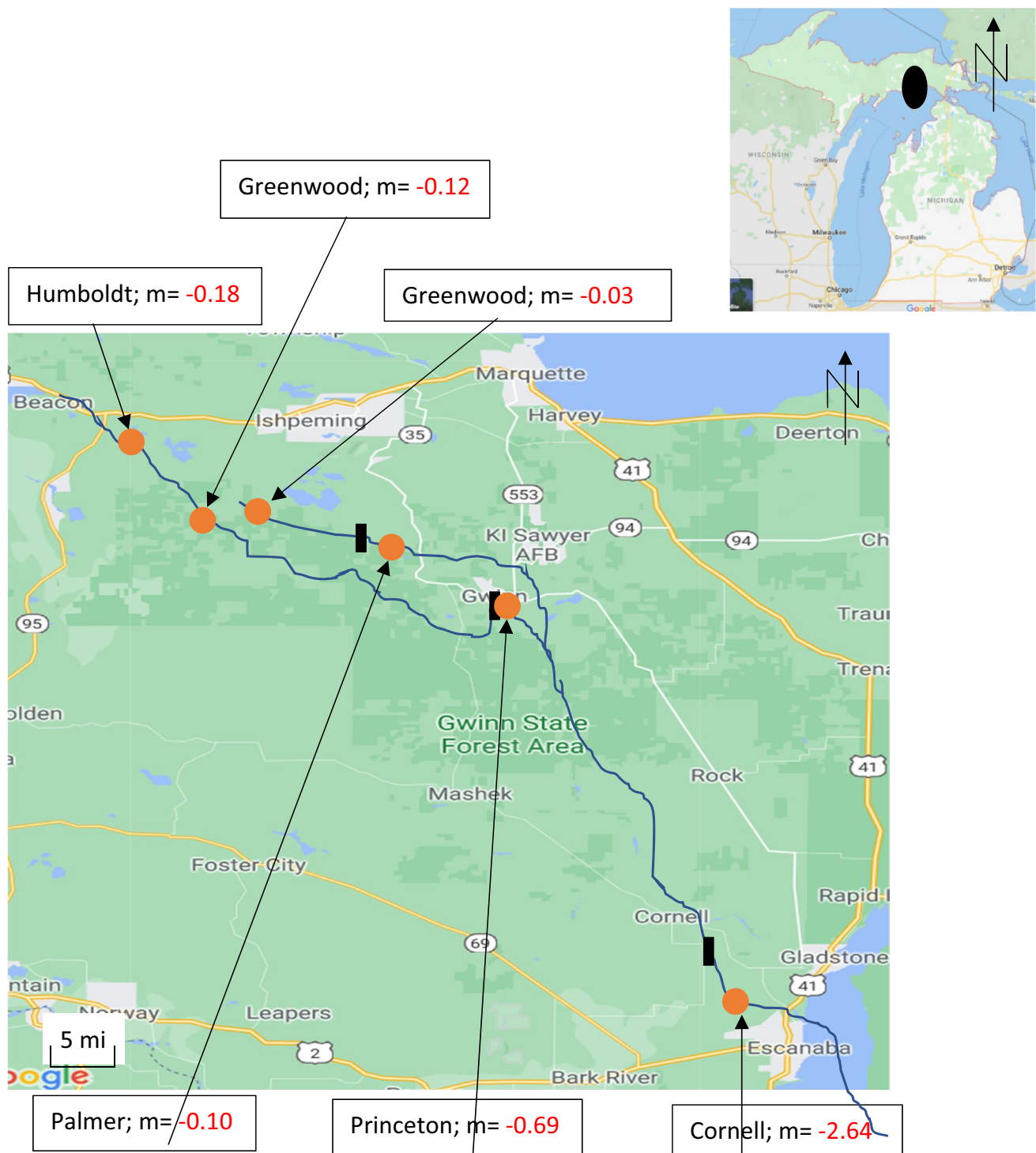


Fig. 12 Escanaba River Basin streamflow with slope of streamflow linear regression, m (Google Maps). The rest can be found in the Supplemental Information (the rivers/streams are blue lines, orange dots represent the streamflow gaging stations, and black rectangles represent dams)

1. The vast majority of gaging locations in Michigan have increasing precipitation (90%) and streamflow (76%).
2. A lower, yet still significant, percentage, of precipitation gage locations have increasing moving standard deviation values (54%).
3. A minority of streamflow gage locations have an increasing moving standard deviation (28%).
4. The hypothesis that precipitation and streamflow are increasing is, therefore, confirmed.

5. The hypothesis that extremes of precipitation are increasing is also confirmed.
6. The hypothesis that extremes of streamflow is not confirmed.
7. Dams and reservoirs help absorb some precipitation from reaching rivers, thereby reducing the possible effects of changing climate on water management.
8. Values of precipitation $P(T \leq t)$ two-tail, precipitation linear regression slope, and streamflow $P(T \leq t)$ two-tail occur in concentrated regions.
9. Water managers may need increased budgets in the future to handle greater streamflow values for flooding, transportation, recreation, and water supply.

Acknowledgements Many thanks to P.D. Barkdoll for help in data collection and analysis.

Author contributions JEM and BDB: all aspects of the project including methodology, statistical analysis, and manuscript wiring, review, and editing.

Data availability statement Data are available upon request from the corresponding author, including data files and report.

Declarations

Conflict of interest On behalf of all authors, the corresponding author states that there is no conflict of interest.

References

- Adib A, Tavancheh F (2019) Relationship Between Hydrologic and Metrological Droughts Using the Streamflow Drought Indices and Standardized Precipitation Indices in the Dez Watershed of Iran. *Int J Civ Eng* 17(7):1171–1181. <https://doi.org/10.1007/s10333-019-00721-6>
- Al-Hasani AAJ (2019) Sensitivity assessment of the impacts of climate change on streamflow using climate elasticity in Tigris River Basin, Iraq. *Int J Environ Stud* 76(1):7–28. <https://doi.org/10.1080/00207233.2018.1494924>
- Ali R, Kuriqi A, Abubaker S, Kisi O (2019) Long-term trends and seasonality detection of the observed flow in yangtze river using Mann-Kendall and Sen's innovative trend method. *Water* 11(9):1855. <https://doi.org/10.3390/w11091855>
- Asarian JE, Walker JD (2016) Long-term trends in streamflow and precipitation in Northwest California and Southwest Oregon, 1953–2012. *J Am Water Resour Assoc* 52(1):241–261. <https://doi.org/10.1111/1752-1688.12381>
- Balistrocchi M, Tomirotti M, Muraca A, Ranzi R (2021) Hydroclimatic variability and land cover transformations in the central Italian alps. *Water (switzerland)*. <https://doi.org/10.3390/w13070963>
- Darlane AB, Pouryafar E (2021) Quantifying and projection of the relative impacts of climate change and direct human activities on streamflow fluctuations. *Clim Change*. <https://doi.org/10.1007/s10584-021-03060-w>
- Fleming BJ, Archfield SA, Hirsch RM, Kiang JE, Wolock DM (2021) Spatial and temporal patterns of low streamflow and precipitation changes in the chesapeake bay watershed. *J Am Water Resour Assoc* 57(1):96–108. <https://doi.org/10.1111/1752-1688.12892>
- Fooladi M, Golmohammadi MH, Safavi HR, Mirghafari R, Akbari H (2021) Trend analysis of hydrological and water quality variables to detect anthropogenic effects and climate variability on a river basin scale: a case study of Iran. *J Hydro-Environ Res* 34:11–23. <https://doi.org/10.1016/j.jher.2021.01.001>
- Gu L, Yin J, Zhang H, Wang H-M, Yang G, Wu X (2021) On future flood magnitudes and estimation uncertainty across 151 catchments in mainland China. *Int J Climatol* 41(S1):E779–E800. <https://doi.org/10.1002/joc.6725>
- Guo L-P, Yu Q, Gao P, Nie X-F, Liao K-T, Chen X-L, Hu J-M, Mu X-M (2018) Trend and change-point analysis of streamflow and sediment discharge of the Gongshui River in China during the last 60 years. *Water (switzerland)*. <https://doi.org/10.3390/W10091273>
- Gupta SK, Gupta N, Singh VP (2020) Variable-sized cluster analysis for 3D pattern characterization of trends in precipitation and change-point detection. *J Hydrol Eng*. [https://doi.org/10.1061/\(ASCE\)HE.1943-5584.0002010](https://doi.org/10.1061/(ASCE)HE.1943-5584.0002010)
- Hagedorn B, Meadows C (2021) Trend analyses of baseflow and BFI for undisturbed watersheds in Michigan-constraints from multi-objective optimization. *Water (switzerland)* 2:221. <https://doi.org/10.3390/w13040564>
- Henn B, Clark MP, Kavetski D, Newman AJ, Hughes M, McGurk B, Lundquist JD (2018) Spatiotemporal patterns of precipitation inferred from streamflow observations across the Sierra Nevada mountain range. *J Hydrol* 556:993–1012. <https://doi.org/10.1016/j.jhydrol.2016.08.009>
- Kelly CN, McGuire KJ, Miniati CF, Vose JM (2016) Streamflow response to increasing precipitation extremes altered by forest management. *Geophys Res Lett* 43(8):3727–3736. <https://doi.org/10.1002/2016GL068058>
- Kuriqi A, Ali R, Pham QB, Gambini JM, Gupta V, Malik A, Linh NTT, Joshi Y, Anh DT, Nam VT, Dong X (2020) Seasonality shift and streamflow flow variability trends in central India. *Acta Geophys* 68:1461–1475. <https://doi.org/10.1007/s11600-020-00475-4>
- Lee C-H, Yeh H-F (2019) Impact of climate change and human activities on streamflow variations based on the budyko framework. *Water (switzerland)* 1:219. <https://doi.org/10.3390/w11102001>
- Leuthold SJ, Ewing SA, Payn RA, Miller FR, Custer SG (2021) Seasonal connections between meteoric water and streamflow generation along a mountain headwater stream. *Hydrol Process*. <https://doi.org/10.1002/hyp.14029>
- Lindström G (1997) A simple automatic calibration routine for the HBV model. *Hydrol Res* 28(3):153–168
- Lucas MC, Kublik N, Rodrigues DBB, Meira Neto AA, Almagro A, de Melo DCD, Zipper SC, Oliveira PTS (2021) Significant baseflow reduction in the sao francisco river basin. *Water (switzerland)*. <https://doi.org/10.3390/w13010002>
- Ma D, Xu Y-P, Gu H, Zhu Q, Sun Z, Xuan W (2019) Role of satellite and reanalysis precipitation products in streamflow and sediment modeling over a typical alpine and gorge region in Southwest China. *Sci Total Environ* 685:934–950. <https://doi.org/10.1016/j.scitotenv.2019.06.183>
- Mallakpour I, Sadegh M, AghaKouchak A (2018) A new normal for streamflow in California in a warming climate: Wetter wet seasons and drier dry seasons. *J Hydrol* 567:203–211. <https://doi.org/10.1016/j.jhydrol.2018.10.023>
- Nkhonjera GK, Dinka MO, Woyessa YE (2021) Assessment of localized seasonal precipitation variability in the upper middle catchment of the olifants river basin. *J Water Clim Change* 12(1):250–264. <https://doi.org/10.2166/wcc.2020.187>
- NOAA (2021) Climate data online help. <https://www.ncdc.noaa.gov/cdo-web/faq#generalSection>. Accessed 15 Mar 2021

- NWS (2021) Michigan climate. National Weather Service, <https://www.weather.gov/media/dtx/prepare/climateLocal.pdf>. Accessed Mar 2022
- Penn CA, Clow DW, Sexstone GA, Murphy SF (2020) Changes in climate and land cover affect seasonal streamflow forecasts in the Rio Grande Headwaters. *J Am Water Resour Assoc* 56(5):882–902. <https://doi.org/10.1111/1752-1688.12863>
- Shrestha RR, Pesklevits J, Yang D, Peters DL, Dibike YB (2021) Climatic controls on mean and extreme streamflow changes across the permafrost region of Canada. *Water (switzerland)* 13:21. <https://doi.org/10.3390/w13050626>
- Sidibe M, Dieppois B, Mahé G, Paturel J-E, Amoussou P, Anifowose EB, Lawler D (2018) Trend and variability in a new, reconstructed streamflow dataset for West and Central Africa, and climatic interactions, 1950–2005. *J Hydrol* 561:478–493. <https://doi.org/10.1016/j.jhydrol.2018.04.024>
- State of Michigan (2021) Does Michigan have the longest coast line in the United States? <https://www.michigan.gov/som/0,4669,7-192-26847-103397--,00.html>. Accessed Mar 2022
- Swain SS, Mishra A, Chatterjee C, Sahoo B (2021) Climate-changed versus land-use altered streamflow: A relative contribution assessment using three complementary approaches at a decadal time-spell. *J Hydrol*. <https://doi.org/10.1016/j.jhydrol.2021.126064>
- Talchabhadel R, Aryal A, Kawaiki K, Yamanoi K, Nakagawa H (2021) A comprehensive analysis of projected changes of extreme precipitation indices in West Rapti River basin, Nepal under changing climate. *Int J Climatol* 41(S1):2581–2599
- Tan X, Gan TY (2017) Multifractality of Canadian precipitation and streamflow. *Int J Climatol* 37:1221–1236. <https://doi.org/10.1002/joc.5078>
- Tan H, Chen X, Shi D, Rao W, Liu J, Liu J, Eastoe CJ, Wang J (2021) Base flow in the Yarlungzangbo River, Tibet, maintained by the isotopically-depleted precipitation and groundwater discharge. *Sci Total Environ*. <https://doi.org/10.1016/j.scitotenv.2020.143510>
- USGS (2021a) How much distance does a degree, minute, and second cover on your maps? https://www.usgs.gov/faqs/how-much-distance-does-a-degree-minute-and-second-cover-your-maps?qt-news_science_products=0#qt-news_science_products. Accessed Mar 2022
- USGS (2021b) Streamgaging Basics. https://www.usgs.gov/mission-areas/water-resources/science/streamgaging-basics?qt-science_center_objects=0#qt-science_center_objects. Accessed 15 Mar 2021
- Vijay A, Sruthi DS, Mudbhatkal A, Mahesha A (2021) Long-term climate variability and drought characteristics in tropical region of India. *J Hydrol Eng*. [https://doi.org/10.1061/\(ASCE\)HE.1943-5584.0002070](https://doi.org/10.1061/(ASCE)HE.1943-5584.0002070)
- Wasko C, Nathan R, Peel MC (2020) Trends in global food and streamflow timing based on local water year. *Water Resour Res* 56:e2020WR027233
- Wen Q, Sun P, Zhang Q, Li H (2021) Nonstationary ecological instream flow and relevant causes in the Huai river basin, China. *Water (switzerland)*. <https://doi.org/10.3390/w13040484>
- Xu ZP, Li YP, Huang GH, Wang SG, Liu YR (2021) A multi-scenario ensemble streamflow forecast method for Amu Darya River Basin under considering climate and land-use changes. *J Hydrol*. <https://doi.org/10.1016/j.jhydrol.2021.126276>
- Yan T, Shen Z, Bai J (2017) Spatial and temporal changes in temperature, precipitation, and streamflow in the Miyun Reservoir Basin of China. *Water (switzerland)*. <https://doi.org/10.3390/w9020078>
- Zeileňáková M, Purcz P, Hlavatá H (2017) Trend detection in precipitation data in climatic station. In: Proc. 10th International Conference on Environmental Engineering, ICEE 2017, <https://doi.org/10.3846/enviro.2017.096>
- Zeng X, Schnier S, Cai X (2021) A data-driven analysis of frequent patterns and variable importance for streamflow trend attribution. *Adv Water Resour*. <https://doi.org/10.1016/j.jhydrol.2021.126294>
- Zhang L, Karthikeyan R, Bai Z, Wang J (2017) Spatial and temporal variability of temperature, precipitation, and streamflow in upper Sang-kan basin, China. *Hydrol Process* 31(2):279–295. <https://doi.org/10.1002/hyp.10983>
- Zhang J, Gao G, Li Z, Fu B, Gupta HV (2020) Identification of climate variables dominating streamflow generation and quantification of streamflow decline in the Loess Plateau, China. *Sci Total Environ*. <https://doi.org/10.1016/j.scitotenv.2020.137935>
- Zhong D, Dong Z, Fu G, Bian J, Kong F, Wang W, Zhao Y (2021) Trend and change points of streamflow in the yellow river and their attributions. *J Water Clim Change* 12(1):136–151. <https://doi.org/10.2166/wcc.2020.144>

Publisher's Note Springer Nature remains neutral with regard to jurisdictional claims in published maps and institutional affiliations.